Proceedings World Geothermal Congress 2010
Bali, Indonesia, 25-29 April 2010

Coupled Geothermal - Hydraulic 3D Modeling of the Southern Vienna Basin. a State of the Art Decision Planning Tool for Sustainable Hydrothermal Exploitation Inside an Environment of Sensitive Hydraulic Circulation Systems.

Goetzl[1] G., Faber[2] R., Janda[1] C., Schubert[1] G. & Zekiri[1] F.

[1]Geological Survey of Austria, A-1030 Vienna, Neulinggasse 38

[2]Terramath, A-3021 Pressbaum, Hauptstrasse 59

Gregor.Goetzl@geologie.ac.at

Keywords: Vienna Basin, Heat Flow Density, Thermal Conductivity, Hydraulic Permeability, Reservoir Modeling

ABSTRACT

Situated at the transition zone of the Eastern Alpine and Carpathian Orogeny, the Southern Vienna Basin marks a region of traditional geothermal utilization in terms of wellness and spa facilities. Geothermal springs, which are strongly related to fault systems at the margin of the basin, are known and used since roman age. Deep wells, primarily executed for hydrocarbon exploration purposes, proofed the existence of far-reaching circulation systems into depths of several kilometers beneath surface. The proximity of the large city Vienna enhances the demand for energetic geothermal utilization for district and agricultural heating purposes. This in fact provokes risks of over-exploitation of natural geothermal systems of the Southern Vienna Basin, which have to be considered as sensitive.

The outcome of the presented study will be represented by steady state physical models (3D) of subsurface temperatures due to conductive and convective heat transport. Based on these calibration models detailed reservoir simulations can be extracted for investigating the thermal influence of future geothermal utilization, and in turn allows to quantify heat- and fluid extraction rates as well as to monitor relevant hydrothermal reservoirs.

The complex lithotectonic build-up of the Southern Vienna Basin leading to several different autochthonous and allochthonous floors, as a result of an altering tectonic evolution, offered particular challenges for geological 3D modeling, which represents the fundament of the executed basin analysis. Furthermore, sparse and partially poorly documented deep wells, which represent the crucial data sources, led to the demand for elaborating statistical and analytical approaches for prediction of rock parameters and thermal boundary conditions. The presented paper intends to give a detailed overview how to deal with numerical hydrothermal analysis based on 3D modeling at complex basin structures at the absence of detailed reservoir information, which may, for example, be derived out of 3D seismic blocks.

1. INTRODUCTION

The southern Vienna Basin is marked out by a long tradition of thermal water use for recreation and health purposes. Almost all existing utilizations have originally been related to natural discharging thermal springs, which are a part of a complex hydrodynamic system (Wessely 1983). Recharged by the nearby outcropping Northern Calcerous Alps (NCA) the thermal water systems may be classified as very sensitive and vulnerable to over-exploitation. The still growing nearby capital city Vienna and the accompanying rising demand on energy supply leads to increased interest on geothermal utilization at the southern Vienna Basin. This may sooner or later cause hazardous impacts on the existing thermal water systems. The fact that the observed hydrodynamic systems are yet not totally understood for flowing paths and quantitative balancing, makes it difficult for public authorities to assign submitted geothermal utilizations grants. Therefore a combined geothermal - hydrological study (acronym Thermalp) has been initiated to provide a better understanding of the thermal water systems of the southern Vienna Basin and to establish a base model for quantitative determination of future water and heat extraction rates for geothermal utilization purposes. Thermalp intends to investigate, outline and classify existing reservoir systems by applying 3D modelling techniques. Starting at a regional scale model covering the most promising structure of the southern Vienna Basin – the so called “Moedling Block” – the elaborated data models will be successively focussed on relevant reservoirs, which shall finally lead to a quantitative decision planning and monitoring tool in terms of a numerical reservoir simulator. Concerning the initial regional data-model special challenges are met due to a complex geological build-up (see also chapter 2.2) and a generally poor data background (see also chapter 3). In contrast to the majority of the present geothermal reservoir studies a detailed data fundament in terms of a 3D seismic block is lacking.

Due to the circumstance that the study Thermalp is still ongoing and will be not accomplished until 2010, the presented paper will be limited to preliminary results and therefore intends to exhibit and discuss the chosen approach.

2. INVESTIGATION AREA

2.1 Geographical Overview

Situated at the eastern part of Austria the Vienna Basin has an extension of approximately 200 km length and max. 50 km width also covering parts of western Slovakia. With a congregation of more than 2.5 million habitants it comprises the largest conurbation of Austria. The investigation area is situated at the southern Vienna Basin, which is confined by the river Danube and the city Vienna (north), the Northern Alps mountains (south and west) as well as the Leitha mountains (east). All present major thermal water utilizations are situated at the investigation area (see also fig. 1), while all known natural thermal- and subthermal water discharges are in turn related to the margins of the southern Vienna Basin.

2.2 Geological Background

Located at the transition zone between the Eastern Alps and the Western Carpathians, the Vienna Basin is a well studied classical pull-apart basin showing the shape of a spindle (Wessely 2006). Its general strike direction is oriented SW – NE, which is related to paleozoic metamorphic bedrocks of the Bohemian Massif (Variscian orogeny) acting as an indenter for Alpine thrusting (Brix and Schultz 1993).

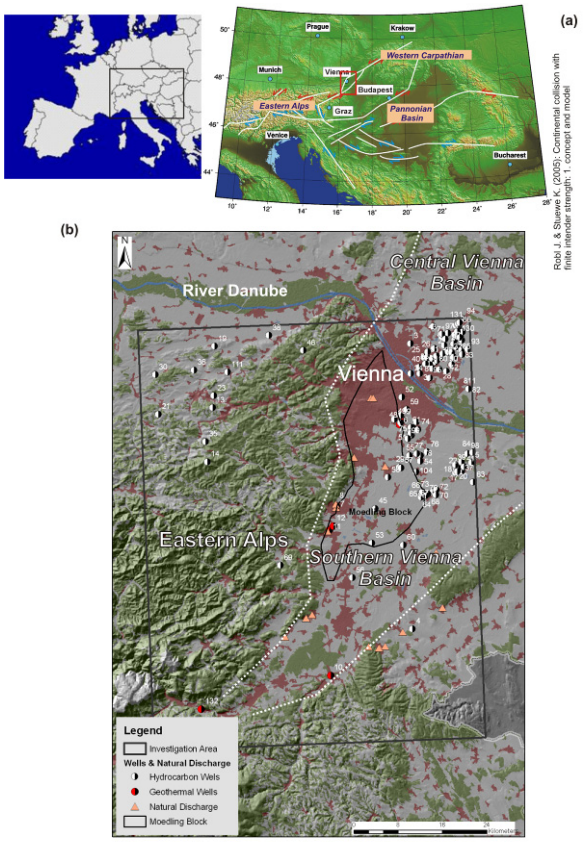

Figure 1: Geographical overview of the investigation area at the southern Vienna Basin. Tectonic position among central European structures (a) and detailed map of the southern Vienna Basin (b) showing the modeling block.

In the area of the Vienna Basin sediments of several stages of deposition are building a pile partly in autochthonous position and partly transported as thrust sheets. The tectogenetic evolution of the Vienna Basin area began with a first phase of subsidence during middle Jurassic time which led to the genesis of a synsedimentary rift basin (Pre-Vienna Basin) and was followed by a more or less stable period of sedimentation from late Jurassic to late Cretaceous (autochthonous Mesozoic sediments). This passive margin basin setting ended with the gradually evolving thrust belt in the south forming a molasse fordeep basin in the north which was partly overthrusted by the Alpine/Carpathian nappes. Evidence for that is provided by exploration wells showing Oligocene molasse sediments below the Alpine nappes at depth of up to 6000m. Tensional forces during ongoing thrusting in the early Miocene led to the development of a piggyback basin on top of the Alpine/Carpathian nappes (Proto-Vienna Basin). Therefore we find today corresponding sediments in the molasse foredeep and in the northern part of the actual Vienna Basin. The last and still ongoing evolutional stage of the Vienna Basin is governed by ceased thrusting and subsidence again since early Miocene age due to pull-apart mechanisms (Neo-Vienna Basin).

As a consequence of this, the Vienna Basin has to be separated into three different main floors: An autochthonous floor consisting of neogene sediments [A] on top, followed by allochthonous Austroalpine and Penninic nappes [B], which in turn have been thrusted onto a basal autochthonous floor consisting of tertiary and mesozoic sediments as well as its crystalline basement [C] belonging to the variscian Bohemian Massif.

The “Neo-Vienna Basin” is split into several high-plateaus and depressions, which are separated by a system of normal- and strike-slip faults (e.g. Vienna Basin Transform Fault-System, Leopoldsdorf- and Steinberg Fault-System). At the main depocenter (Zistersdorf Depression) neogene basin fillings reach thicknesses of up to 5000 meters.

The southern Vienna Basin is characterized by a central, tectonically active rift system (Wiener Neustadt Depression, Mitterndorf Depression), which is flanked by high-plateaus at the western (Moedling Block) and eastern margin of the basin. Heading northwards, the central rift system passes into a major depocenter (Schwechat Depression) showing neogene basing fillings of up to 4000 meters. Separated by the Leopoldsdorf Fault System, the Schwechat depression opposites the thermal water bearing so called “Oberlaa High” structure, which is related to Neogene basin depths of less than 500 meters below surface.

2.3 Hydrological Background

In general the Vienna Basin exhibits two different main types of thermal water systems: Locally more or less confined and partially overpressured brines without alimentation [a] and in contrast actively recharged hydrodynamic systems showing low to moderate salinity [b]. While aquifer type [a] is widely spread across the entire Vienna Basin and can be encountered both in permeable neogene sediment layers and cropped basement reservoirs of the central depressions, system [b] is limited to high plateaus at the southern margins of the basin.

The Moedling Block at the western margin of the southern Vienna Basin covers, as already mentioned, the most relevant hydrodynamic thermal water systems. Following a concept published by Wessely (1983) the main recharge area is located west and southwest of the Vienna Basin and is related to high permeable, partly karstified upper and middle Triassic dolomites and limestone (Hauptdolomit, Wetterstein Schichten), which are continued to the basement of Moedling Block (see also Figure 2).

The hydrodynamic systems of the Moedling Block are supposed to be limited by the Leopoldsdorf Fault System toward east direction. This fact is clearly indicated by high mineralized, connate formation fluids trapped at analogue permeable basement rock of the Schwechat Depression, which is located beyond the Leopoldsdorf Fault System (q.v. Figure 2 and Figure 4). Toward north direction the Moedling Block hydrodynamic system is limited by impermeable formations belonging to the Penninic Flysch Zone (mostly interbedded silt-, sand- and clay stones). In turn slates and quartzites belonging to the Upper Austroalpine Greywacke Zone act as limiter toward south direction.

The Moedling Block hydrodynamic system itself can be split in at least 3 different sub-systems, which are mainly related to the major nappes and, presumably, major fault systems. The different subsystems mainly differ in mineral

content (especially sulfide content), which is a consequence of varying hydrodynamic circulation lengths inside the carbonatic nappes. The more so as trapped natural thermal water at the sites “Baden” and “Bad Voeslau”, which are separated by only a few kilometers show totally different contents of hydrogen sulfide (Zoetl and Goldbrunner 1993).

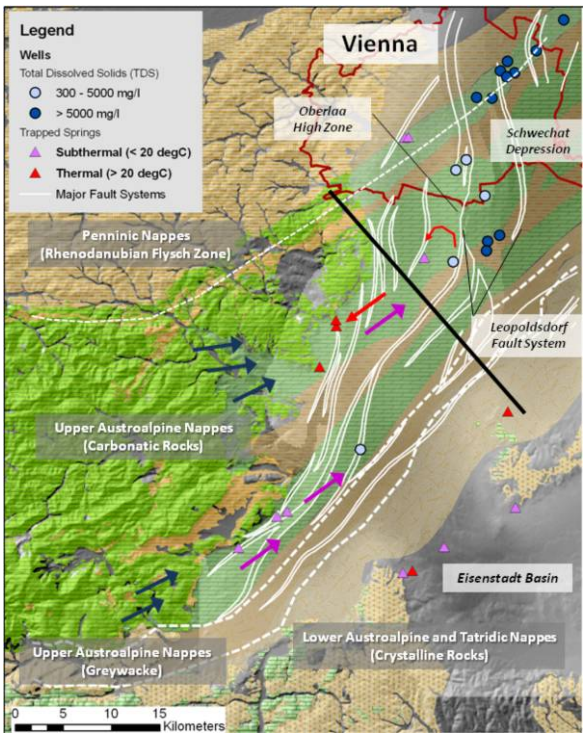

Figure 2: Hydrogeological map of the investigation area using a simplified 2 color scheme. Permeable units, predominately consisting of Triassic carbonates are colored green. Orange colored sections cover impermeable to low permeable, mostly sedimentary and crystalline rocks. Hydrodynamic circulation paths are indicated by colored arrows. The black line represents the location of a hydrogeological cross-section through the southern Vienna Basin (q.v. Figures 3,4).

In general, internal fault systems are supposed to play an important role for the development of infiltration- and exfiltration paths leading to maximum hydraulic infiltrations depth of more than 4000 meters below surface (e.g. Well #69). As observed at several wells, conglomeratic Neogene layers (e.g. “Aderklaa Formation”, ”Rothneusiedel Formation”) are partially hydraulically connected to often karstified, high permeable top-layers of the carbonatic basement and provide discharge toward the margins of the southern Vienna Basin.

2.4 Geothermal Background

The overall geothermal conditions at the region of the Vienna Basin are influenced by the Alpine Orogeny, the still continuing subsidence of the Vienna Basin itself as well as by the Pannonian Basin. Superimposed by locally confined anomalies due to infiltrating and discharging water systems, observed surface heat flow densities vary quite strongly within the range of 40mW/m² to 95mW/m² (see also chapter 5.4). In general, reduced geothermal conditions towards the Northern Calcerous Alps (western part of the investigation area) are related to crustal stacking in combination with enhanced surface water inflow. In opposite to this geothermal conditions are successively elevated toward the south-eastern part of the investigation area, which is a consequence of crustal thinning at the Pannonian Basin. Heading toward the north- eastern part of the Vienna Basin generally reduced heat flow densities are observed which is assumed to be a consequence of thermally non steady-state conditions due to intense deposition of cold surface sediments.

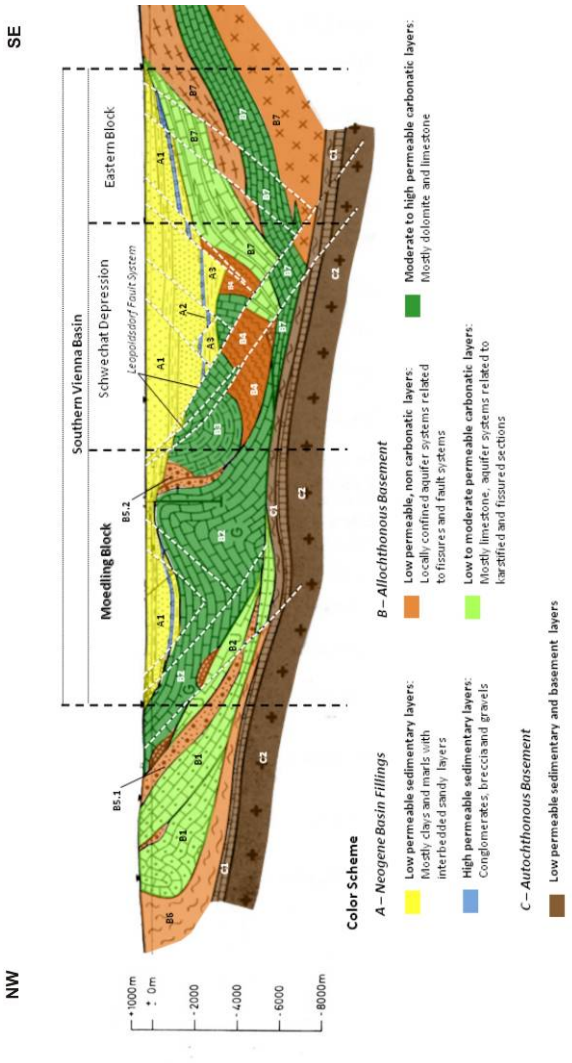

Figure 3: Simplified hydrogeological cross-section through the Southern Vienna Basin (Wessely 1983, modified) showing main structures as well as generalized formations, which are displayed at the 3D geometrical model.

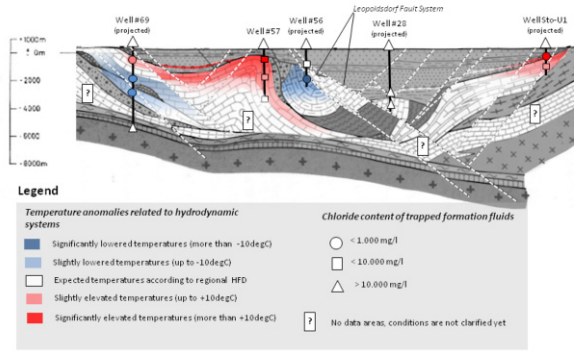

Figure 4: Temperature and hydro-chemical anomalies related to the southern Vienna Basin hydrody-

namic systems, projected on the cross section shown at Figure 3.

At high permeable, widely karstified zones within carbonatic units of the Northern Calcareous Alps infiltrating meteoric water is verifiable lowering the local temperature regime up to depths of at least 4000 meter below surface (see also Figure 4). In opposite to this clearly elevated surface heat flow densities have been observed at discharge areas of the same hydrodynamic systems, which are often only separated by some 10^0 to 10^1 km in horizontal direction leading to low scale heat flux patterns.

3. DATA BACKGROUND

Unlike to many recent 3D geothermal resource-mapping studies the presented project is not able to fund on detailed 3D seismic data. In order to establish a first-approach regional 3D data-model of the southern Vienna Basin focusing the coupled geothermal hydraulic regime, the following general classes of data-sets are needed (see also chapter 4):

- Geometrical and structural data describing the volumetric extend of relevant hydrogeological units.
- Structural in-situ information gained from borehole-logging for internal hydraulic zoning of relevant hydrogeological units.
- Petrophysical data (thermal, hydraulic properties) for model attribution.
- Hydro-chemical and hydrologic data for hydraulic balancing of the investigation area.
- Thermal data (borehole- and outflow temperatures, HFD data) for model calibration.

Except the previously described hydrodynamic concept of Wessely (1983) and geological base maps, comprehensive compilations of petrophysical, hydrologic and geothermal datasets have initially been widely lacking for the Southern Vienna Basin.

3.1 Data Sources

Due to fact, that the southern Vienna Basin generally represents a region of hydrocarbon prospection, hydrocarbon wells exhibit the most relevant data-sources at the investigation area. In total the investigation area comprises around 130 wells, which are unfortunately situated quite unbalanced focusing the more prosperous north-eastern part of the southern Vienna Basin. Inside the Moedling Block and west of it only a few wild-cats as well as around 10 thermal-water exploitation wells are available. The structural interpretation of existing 2D seismic data is generally limited to the Neogene basin. For that reason structural- and geological information had to be additionally taken from different surface- (Schnabel 2002) and basement maps (Kroell 1993) at a scale of 1:200.000 as well as from various existing geological cross sections, which are of quite heterogeneous quality and therefore partially contradictory.

3.2 Additional Field and Laboratory investigations

Additional field- and laboratory measurements are concentrated on petrophysical and hydro-chemical measurements.

Thermal rock parameters, such as effective heat conductivity, heat capacity and radiogenic heat production rates have not been studied before at the Vienna Basin. Based on available drilling cores from hydrocarbon wells laboratory measurements are executed to acquire the above mentioned parameters. Following the chosen approach for modeling thermal conductivities and heat capacities, which is described at chapter 4.2, the executed laboratory measurements are designed for estimation of pure solid matrix-properties. For that purpose rock samples will be investigated at different state of fluid saturation (air, fresh-water and brine) in combination with measurements of the total pore-fraction, which in turn allows extrapolating matrix-attributes.

The additional hydro-chemical field investigations intend to outline the different hydraulic circulation systems and subsystems at the southern Vienna Basin as well as related circulation paths. In this context emphasize is also set on the possibility of trans-circulating aquifer systems between the western and eastern margin of the southern Vienna Basin (see also Figure 3 and Figure 4). Based on natural discharging and trapped thermal and sub-thermal waters the currently executed investigations therefore focus on isotope measurements (O^{18}, S^{35}, H^3 and C^{14}) in order to distinguish between different circulation systems and to identify different levels of mixing with fresh surface waters.

4. APPROACH AND METHODOLOGY

The presented study intended to establish a geothermal 3D model, which is possible to regard advective heat flow related to active water circulation. As a first approach a model will be elaborated at a regional scale focussing a promising hydrodynamic active structure of the southern Vienna Basin, the so called Moedling Block. The regional model intends to outline relevant aquifer systems and to quantify circulation rates. The lack of comprehensive and entire area-wide basic data (petrophysical-, hydraulic-, geological-) requires the elaboration of simplified data-models, which nevertheless allow accurate predictions of a coupled geothermal – hydraulic regime. The thermal simulation will be executed using the finite-element software FRACture™ (Geowatt AG, Switzerland). By the help of iterative refitting of the chosen petrophysical and hydraulic modelling parameters in order to derive optimum input values, which will be achieved by comparison of modelled subsurface temperatures and hydraulic conditions (discharge rates and water pressure) with measured ones. The subsequently following sub-chapters will provide an outline of the main tasks to reach this goal.

4.1 Geological Modeling

The coupled thermal – hydraulic modeling bases on a geometrical 3D model, which mainly regards hydro-geological aspects and expected contrasts of thermal conductivities. Due to the fact, that the once defined volumetric model cannot be refitted after discretization into a finite-element grid for numerical modeling, emphasize had to be set on the generalization of geologic units. Referring to the existing geological maps as well as to geological logs of the investigated deep-wells, the investigation area exhibits more than 500 individual geological units, which had to be generalized to 13 formations in order to enable clearly-arranged geometrical modeling using the software package Geomodeller™ (Intrepid Geophysics, AUS). Limitations of the software as well as a heterogeneous data distribution in combination with a complex tectonic setting and partly contradictory geological information in a variety of scales have made this selection challenging. The generalization has been executed stepwise in regard to expectable contrasts in effective thermal conductivities and hydraulic permeabilities and not primarily to formations and tectonic contacts.

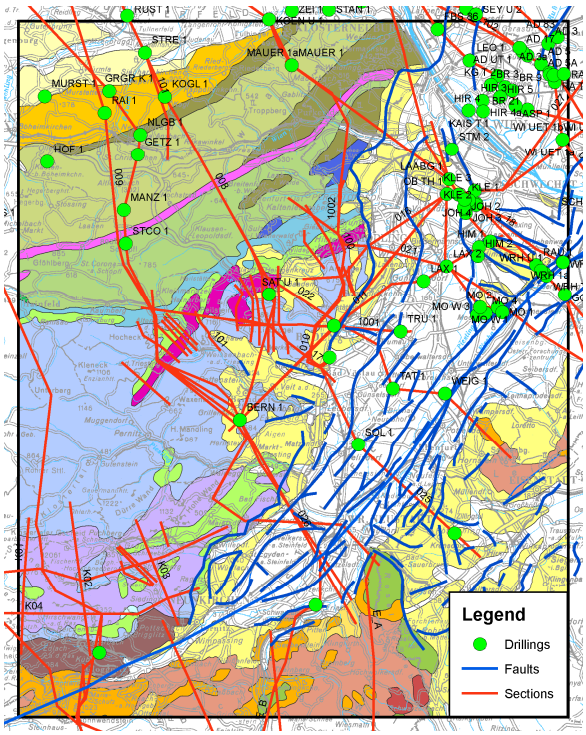

Figure 5: Available input data for modelling.

Geomodeller™ has been chosen because it deals best under these conditions. Other 3D modeling software generally would be more appropriate using seismic data in a "simple" basin environment where it is sufficient to interpolate horizons. In our complex case, lacking seismic data, we need a method which is optimized for our input data and is able to interpolate the geology by taking this data into account. The potential-field interpolation algorithm of the software meets these criteria best (Calcagno et al 2008).

Based on the generalized stratigraphic pile (Table 1) all relevant geological input data were revised and assigned to the according formations. In this way a geological map, around 20 cross sections, dip values and more than 100 borehole data were imported.

In addition to the above mentioned data a generalized and strongly reduced set of faults was integrated into the 3D-Geomodeller. To respect the feasibility of the software and the harmonized geological data only a few faults with simple geometry on the border of the basin have been incorporated and complex fault networks and geometries (flower structure) neglected.

Modeling itself is done stepwise from the base to the top layer. The resulting 3D model will then be exported and used for ongoing thermal simulation by Geowatt.

Parallel to the usage of GeoModeller a joint development (TerraMath / GBA) of a 3D Interpolation tool based on TerraMath WinGeol™ have been conducted with the target to add several missing features like:

- Estimation of interpolation quality – respectively the plausibility of the geometrical model
- Support for anisotropic rock properties which is of high importance to later added petrophysical data-model.
- A fully 3D data editor which eases especially the construction of fault surfaces from very heterogeneous data.
- The software design allows later modifications to support multiprocessor computers or cloud computing in a very straightforward way.
- Very simple voxel data structure and is therefore flexible to import to other software packages.

The base algorithm is an inverse distance vector interpolation approach where input vectors with a negative z value are interpreted as overturned strata. The vectors represent the 3 axis of an anisotropy ellipsoid where the primary axis is located parallel to the dipping of the strata. It is assumed that the geometrical simplest solution is in general the most likely – in other words the bending of the strata between the input points is - under consideration of the anisotropy information - minimized. In a second calculation cycle the calculated vector voxel set is filled with lithological information. It is assumed that the anisotropy ellipsoids represent the probability with witch lithological information can spread in a certain direction. This technique does not necessarily require that any input points are located on strata boundaries and is therefore adequate for volumes with poor input data quality as well. This additional modeling approach will be applied to allocate anisotropic, strike- and slip angle depending rock parameters such like thermal conductivity and hydraulic permeability (for data example see also Figure 6).

4.2 Petrophysical Data-Model

Heat- and fluid transport is generally governed by the following material parameters:

(a) Thermal conductivity [solid, fluid and bulk]

(b) Specific heat capacity [solid, fluid and bulk]

(c) Bulk porosity

(d) Bulk density

(e) Hydraulic permeability, effective porosity

(f) Radiogenic heat production rate

While parameters (c) to (e) could in general be derived from existing borehole data, generalized prediction models of effective bulk values (porous rock mass) had to be defined for (a) and (b) due to the lack of already existing data compilations. As a first step generalized lithological models have been designed, based on the simplifying assumption, that all involved individual rock types are distributed homogenously inside a specific stratum. The achieved lithological models have been derived from petrografical drilling-core analyses and relevant literature (Wessely 2006, Faupl 2003). Specific values of (a) and (b) for the involved, specific rock types have preliminary been driven from a compilation of literature data (Kutasov 1999, Schoen 1983). The resulting values for solid rock mass at an ambient temperature of 20 degC have been calculated by weighted arithmetical and geometrical averaging:

$$\lambda_s = \prod_i \lambda_{s,i}^{n_i}$$
$$c_{p,s} = \sum_i c_{p,s,i} \cdot n_i \qquad (1)$$

Geometrical averaging, applied on the calculation of heat conductivities for specific solid strata (1) allows to generally consider anisotropic behavior in an estimative leading to λ_s:: $\lambda_{s,min} < \lambda_s < \lambda_{s,\,max}$. Anisotropy rates of solid heat conductivities have not been modeled, but derived from additionally executed laboratory measurements on distinctive drilling cores. These measurements also serve to refit modeled data of (a) and (b) relating to solid strata (see also chapter 4.2). The dependency of the thermal conductivity on the ambient temperature has been regarded using the following, empiric approach by Sass et al. (1992).

$$\lambda_{\text{eff}}(T_{\text{Form}}) = \frac{\lambda_{\text{eff}}(0°\text{C})}{1.007 + T_{\text{Form}} \cdot \left(0.0036 - \frac{0.0072}{\lambda_{\text{eff}}(0°\text{C})}\right)} \quad (2)$$

In a terminal modeling step effective values of parameter (a) and (b) have been calculated regarding bulk porosities and pore-fluids.

$$\begin{aligned} \lambda_{eff} &= \lambda_s(T)^{(1-\phi_b)} \cdot \lambda_f{}^{\phi_b} \\ c_{p,eff} &= c_{p,s}(T) \cdot (1-\phi_b) + c_{p,f} \cdot \phi_b \end{aligned} \quad (3)$$

For the calculation of effective thermal conductivities and heat capacities (3) two different temperature-invariant fluid-models have been used: Fresh water [λ_s*: 0.68 W/(m·K)*; $c_{p,s}$*: 4128 J/(kg·K)*] for permeable strata and brine [λ_s*: 0.68 W/(m·K)*; $c_{p,s}$*: 3863 J/(kg·K)*] for low- and impermeable layers. Static, stratum related values of bulk porosities have been derived from existing borehole logging data (drilling core analyses and log interpretation). As shown in chapter 5.2 the static, depth-invariant porosity models are able to fit measured borehole data in a sufficient approximation. In a similar manner static, averaged values have for parameters (d) and (f) have been derived from existing borehole logging data and additional measurements.

More structured data-models have been elaborated for parameter (e). Based on effective porosities and hydraulic permeabilities, derived from existing drills-stem tests (DST) and existing core analyses different empiric, depth dependent (relating to the specific relative position inside a specific stratum) models have been elaborated for the main hydro-geological units of the volumetric 3D model (see also chapter 5.2).

The petrophysical data-model was established irrespectively of the volumetric 3D model and later joined to the finite-element grid in order to allow later refitting. Especially at areas of enhanced permeability, as for example the top of carbonatic basement or the close vicinity of believed permeable fault-systems, the resolution of the petrophysical data is clearly increased. Due to the large dimension of the modelling area, all investigated hydro-geological units are treated as porous aquifer systems ignoring internal distribution of discrete, low scale fractures.

4.3 Hydraulic Modeling

An important input for the geothermal model is given by the thermal water convection developed in the Calcareous Alpine within the Moedling Block (see chapter 2.3). At the western margin of the southern Vienna Basin, there exist several thermal springs and wells which discharge the thermal aquifer systems of the Moedling Block. Among them are the spas of Bad Fischau, Bad Vöslau, Baden and Oberlaa. The mean total discharge of the thermal spas amounts around 300 l/s.

In order to distinguish the different thermal aquifer systems, the spas are monitored during the project. This concerns yield and temperature as well as the hydrochemical and isotope hydrological compositions of trapped waters. Based upon these data, the ratio of distinguishable components should be calculated.

Furthermore based on rough hydraulic calculations the mean permeability of the different aquifer systems should be estimated – as additional input for the petrophysical data model.

4.4 Thermal Data Processing

Measured borehole temperatures provide essential thermal information for refitting and interpretation of the coupled thermal- and hydraulic 3D simulation and therefore need to be as plausible as possible. Despite of a few measured outflow temperatures of geothermal wells inside the investigation area, the necessary temperature data are provided by bottom-hole temperature (BHT), drill stem tests (DST) as well as by continuous borehole measurements at hydrocarbon wells. Most of the existing wells have been drilled and tested during the 1960's and 1970's as borehole temperatures have been of minor interest for the oil industry. For that reason the quality of data documentation, in particular the logging of shutdown and circulation periods before BHT measurements is generally poor. Due to the circumstance, that most available temperature logs inside the investigation area are not interpretable, thermal data processing have been focused on quality evaluation of DST datasets and BHT correction. Other data-correction steps, like topographical- or paleoclimatic corrections don't have to be applied as these are automatically considered at the numerical simulation.

The executed BHT corrections followed two different approaches, which had been applied subsequently. As a first step line-source related graphical BHT corrections have been used based on standard methods by Lachenbruch and Brewer (1959) as well as on a modified Horner method by Fertl and Wichmann (1979). Subsequently a numerical BHT correction (cylindrical source) has been applied following a method by Leblanc et al. (1981).

$$T_{\text{Form}} = \text{BHT}(t) - \Delta T' \left[\exp\left(-\frac{a^2}{4\kappa t} \right) - 1 \right] \quad (4)$$

Based on equation (4) a numerical optimization algorithm for at least two individual BHT values have been derived in order to estimate the true, thermally undisturbed formation temperature subjected to optimized values of the bulk thermal diffusivity. The later term also acts as a kind of plausibility control of the achieved result as the bulk diffusivity has to be in between a data interval of $0.15 \cdot 10^{-7}$ m²/s (pure water) and approximately $15 \cdot 10^{-7}$ m²/s (pure rock mass). This method generally leads to stable results, while main processing inaccuracies are related to continued mud circulation inside the well (which is ignored by this approach) and uncertainties in estimating the shutdown period, which was the main source of error during the presented study. Based on assumptions of the bulk thermal diffusivity equation (4) have also been adapted for the correction of single BHT values, which in fact was more sensitive to correction failures.

4.5 Geothermal Modeling

Pure conductive as well as coupled conductive – advective numerical modeling marks a crucial processing step in or-

der to delineate and interpret existing natural hydrodynamic systems inside the investigation area. Geothermal modeling is executed either one-dimensional for estimation of background heat flow densities (HFD) and quality evaluation of measured temperature data as well as in a three-dimensional way in order to simulate the thermal influence of a supposed hydrodynamic circulation system.

4.5.1 Simplified 1D Modeling

Simplified geothermal 1D modeling follows a pure conductive approach based on Fourier's Law ignoring internal, radiogenic heat sources. Terrestrial heat flow is limited to pure radial (z) direction.

$$q = \lambda \cdot \frac{\partial T}{\partial z} \tag{5}$$

Equation (5) can be transformed into a progressive algorithm describing the temperature field of a layered half-space obtaining individual values of effective heat conductivities.

$$T_{i=1,n} = T_{i-1} + q \cdot \frac{m_i}{\lambda_{eff,i}} \tag{6}$$

By interpolation of surface temperatures ($T_{i=0}$) based on soil temperature measurements at different elevation-levels equation (6) can in turn be derived to an iteratively applied inverse algorithm optimizing R = ($T_{meas} - T_{calc}$) by variance of the terrestrial HFD (q). At the chosen optimizing algorithm a constant depth increment (Δz) of 1 meter has been applied in order to establish preferably accurate correction of the temperature dependence of the effective heat conductivity (see also chapter 4.2). The inverse determination of terrestrial HFD values has been applied on all boreholes which obtained interpretable temperature information (DST-, corrected BHT data). The derived temperature-residuals (R) have been interpreted in order to evaluate the plausibility of the available temperature data and in order to estimate possible thermal influences of advective heat flow in a first approach. This was done by calculation of effective Peclet numbers.

$$\mathrm{Pe} = \frac{l \cdot v_{D,z} \cdot \rho_f \cdot c_{p,f}}{\lambda_{eff}} = \frac{\lambda_{equ}}{\lambda_{eff}} - 1 \tag{7}$$

Based on observed temperature-residuals equivalent heat conductivities, influenced by advective heat flow are computed for depth-intervals between measured borehole temperatures (thermal nodes). Equation (8) this leads to the estimation of hydraulic transmissivities (effective hydraulic thickness x Darcy velocity).

4.5.2 Coupled 3D Modelling using FRACTure™

The applied thermal- hydraulic 3D modeling is executed by the help of the finite-element simulation tool FRACTure™ (Geowatt AG, SUI). Originally developed for engineering of stimulated fractured reservoirs (EGS method) at the experimental site Soultz sous Forêts (FRA), FRACTure is able to compute physical coupling of individual thermal and hydraulic transport mechanisms (heat diffusion, convective heat flow) at steady state as well as at transient conditions regarding heterogeneous time scales. The coupled thermal-hydraulic modeling is mathematically based on a generalized heat-balance equation (Kohl and Hopkirk, 1995).

$$\underbrace{\langle \rho c_p \rangle \frac{dT}{dt}}_{\text{transient}} = \underbrace{\mathrm{div}(\lambda \mathrm{grad} T)}_{\text{diffusion}} - \underbrace{[\rho c_p]_f \, v_D \mathrm{grad} T}_{\text{advection}} - \underbrace{A}_{\text{heat-source}} \tag{8}$$

Based on a finite-element grid (model size approx. 40km x 30km x 15km) of varying cell size showing increasing resolution towards existing wells and internal discontinuities (permeable fault systems and layer-boundaries) several simulation-cycles will be executed iteratively in order to optimize the chosen constraints. In a first approach a pure diffusive either steady state as well as transient (regarding paleoclimatic variations) thermal model will be executed in order to evaluate the influence of the surface relief and paleoclimatic variations on the recent geothermal regime. For that purpose model validation will be applied on measured borehole temperatures. Simulation-cycle 1 also intends to refit and reallocate the a-priori postulated values of effective heat conductivities and specific heat capacities. Following an approach, presented at the previous chapter, Peclet analyses based on equation (7) are executed too in order to evaluate and refine assumed high permeable layers.

In subsequent modeling cycles, advective heat flow due to thermal water circulation will be implemented to the simulation. Keeping the hydraulic boundary conditions invariant (water level, recharge- and discharge rate) hydraulic rock parameters (hydraulic permeability) will be iteratively refitted and reallocated by opposition to both measured borehole temperatures and hydraulic pressures. The achieved results are expected to three-dimensionally confine active hydrodynamic circulation zones. This in turn will provide the fundament for later following detailed reservoir models of distinctive reservoirs for sophisticated engineering.

5. PRELIMINARY RESULTS

The coupled thermal- hydraulic 3D modeling is still in progress. For that reason the following chapters intend to examine the elaboration of boundary and subdomain parameters, which have to be understood as start-up values for iterative model refitting. As mentioned above the lack of profound seismic data as well as the scattered distribution of deep boreholes marks special challenges for the prediction of subsurface settings.

5.1 Geological Model

More than 500 individual and partly redundant geological units, gained from borehole logging and geological surface maps have been iteratively generalized to finally 14 main model units covering the entire investigation area (see also Table 1) due to operational limitations of the applied geological modelling software (Geomodeller – Intrepid, AUS).

Table 1: Overview of geometrical model-units.

Model Unit	Name	Main tectonic Units	Time Period	Basin Floor
A1	Neogene Sediments i.g.	Neogene Basin Fillings	Miocene to Holocene	[A] Neogene Basin
A2	Neogene Conglomerats			
A3	Lower Neogene Units			
B1	Bajuvaric Nappes	Upper Austroalpine	Middle Triassic to Lower Cretacous	[B] Allochtonous Basement
B2	Tirolic Nappes		Lower Triassic / Permian to Jurassic	
B3	Juvavic Nappes			
B4	Greywacke Zone		Paleozoic	
B5.1, B5.2	Gosau Group		Upper Cretacous to Eozene	
B6	Flysch Zone	Penninic Nappes	Lower Cretacous to Eozene	
B7	Lower Austroalpine and Tatridic Units	Lower Autroalpine and Tatridicum	Palezoic to Upper Triassic	
C1	Molasse Basin	Bohemian Massif	Eocene to Miocene	[C] Autochthon. Basement
C2	Crystalline Basement		Paleozoic	

The generalized hydrogeological legend clearly focuses on the targeted hydrodynamic system of the so called

Moedling Block and generally neglects possible thermal water circulation systems at the eastern margin of the southern Vienna Basin (see also Figure 3 and Figure 4).

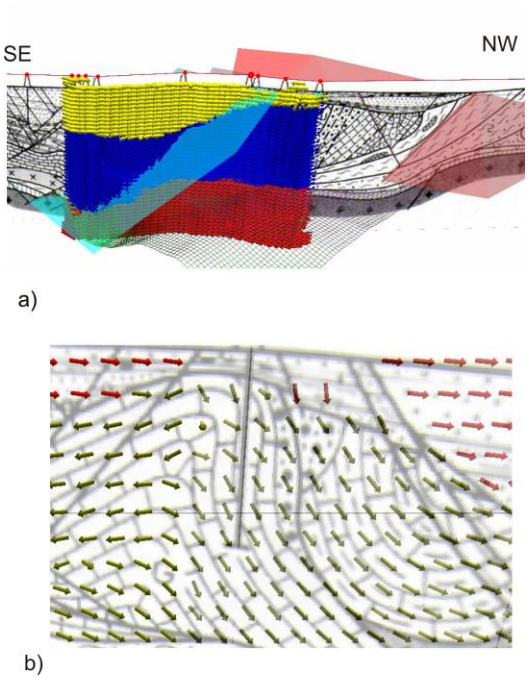

Figure 6: [a] volumetric model of major tectonics section of the southern Vienna Basin along NW – SE striking section using the alternative approach. [b] Detailed view on modelled layer dips (coloured arrows) compared with the above mentioned geological cross-section.

Figure 6 shows the distribution of modelled internal dips associated to generalized model units. This has been achieved using the alternative modelling approach described at chapter 4.1. Based on discrete dipping information, gained from well observation and drawn from existing cross-sections the chosen approach is capable to map internal structures in a sufficient way. Based on volume covering dip information anisotropic behaviour of thermal conductivities and hydraulic permeabilities can be considered.

5.2 Petrophysical Data-Models

The above described geometrical model units have been assigned to petrophysical subdomain parameters gained from pure synthetic modeling (thermal conductivity and heat capacity) as well as from empiric observations (hydraulic permeability, pore fraction and bulk density). Main focus has been set on an adequate prediction of effective thermal conductivity and hydraulic permeability (Figure 7).

Effective thermal conductivity is mainly depending on lithological composition, total pore fraction and related pore fluids. In total 41 individual rock-types (e.g. sandstone, limestone, marl) derived from petrographical analyses applied on drilling cores have shown to be completely sufficient to describe all observed geological formations. Further enhancement in the modeling of the pure solid-matrix behavior will be achieved after accomplishment of laboratory measurements. Preliminary results, gained from measurements on dried rock samples indicate a good conformance between measured and predicted values (see also chapter 5.4). Different methods have been tested in order to model total pore-fraction for the calculation of effective thermal parameters. Emphasize had to be set on the depth-dependence of the total porosity, respectively the decrease of porosity with increasing overburden pressure.

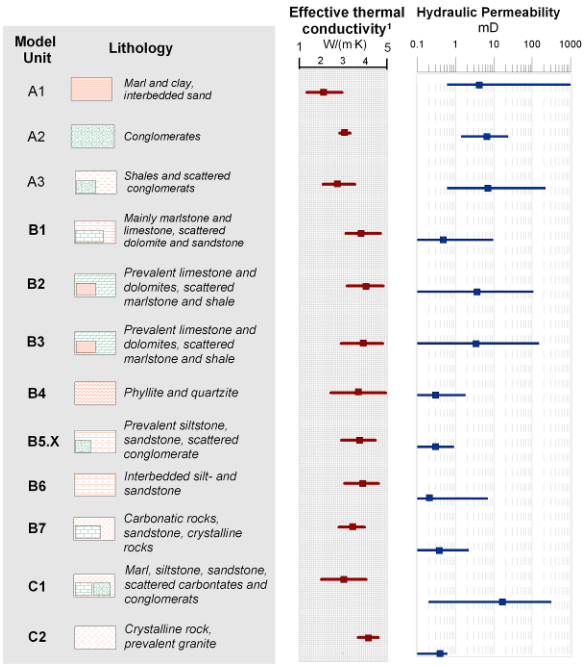

Figure 7: Main petrophysical attributes (starting values and variance) of the generalized geometrical model units.

Based on empiric datasets provided by drilling core measurements and geophysical borehole measurements different models have been elaborated and tested (mainly based on exponential decrease with increasing depth). As shown at Figure 8 a static model of the total pore fraction based on averaged values allocated to individual geological units was completely sufficient to consider dependence on overburden depth, as these values already imply increasing overburden pressure.

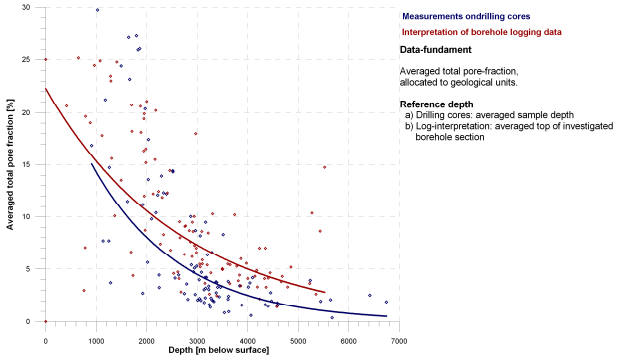

Figure 8: Depth-dependence of averaged total pore fractions allocated to geological units inside the investigation area.

A similar approach has been chosen in order to predict geometrical dependence of hydraulic permeabilities for relevant model units (A3, B1, B2 and B3). Well logs as well as hydraulic drill stem tests indicate discrete zones of enhanced hydraulic permeability at the top sections of carbonatic basement layers (karstification) as well as on the base of Neogene sediments (conglomeratic layers). In a first processing step the expected data range has been statistically derived by using different quantils (median value and 95th percentile). In a next step analyses based on available

well data have been accomplished in order to vertically confine zones of enhanced permeabilities.

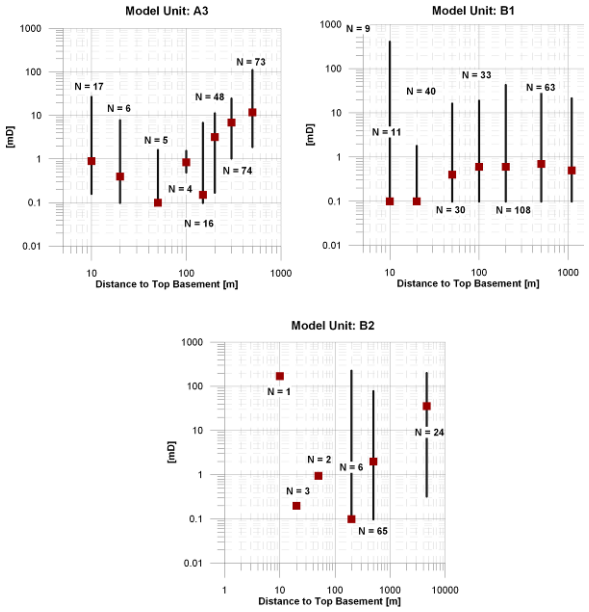

Figure 9: Statistical internal zoning of observed hydraulic permeabilities in order to confine zones of elevated water transfer. Red squares represent median values and top values are limited by the 95th percentile.

Based on existing well data an internal zoning of hydraulic permeability has been applied using the above described statistical values. Unfortunately the vertical distribution of measured data is rather unbalanced, especially for model unit B2 and B3 (q.v. Figure 7). These model units are assumed to be the most important aquifers of the investigation area. Nevertheless the available data show evidence for slightly enhanced permeable layers inside unit A3 at the first 20 to 50 meters above basement (q.v. Figure 9). Furthermore model unit B2 exhibits highly permeable layers at more than 1000 meters below the top of the generalized unit.

5.3 Thermal Model

As a first investigative step simplified thermal 1D modeling, based on pure conductive heat transport, has been applied on wells with existing temperature information. A numerical inverse optimization algorithm, which has been described at chapter 4.4 has been applied in order to determine the overall surface heat flow density as well as resulting residuals between measured and modeled subsurface temperatures for each individual well. These significant values in turn allow accomplishing a quality check of available temperature data as well as gaining an overview of the regional geothermal regime.

In total 87 wells have been investigated showing an average surface heat flow density of 72.8±11.5 mW/m². The executed inverse modeling was calibrated on 372 discrete temperature measurements, which have mainly been gained at the course of hydraulic drill stem tests. Additionally corrected BHT data based on both multiple and single BHT measurements at a specific depth have been considered as well for the modeling. Unfortunately these nodes turned out to be insufficiently accurate in most cases due to poor data documentation and have therefore been ignored. In general the average model fitting is in the range of 2.7 K. Keeping in mind that the preliminary chosen approach is not able to consider advective heat transport and the available temperature data generally obtain an accuracy of 1 K, the observed residuals seem to be acceptable for a first approach toward the description of the regional geothermal regime of the investigation area.

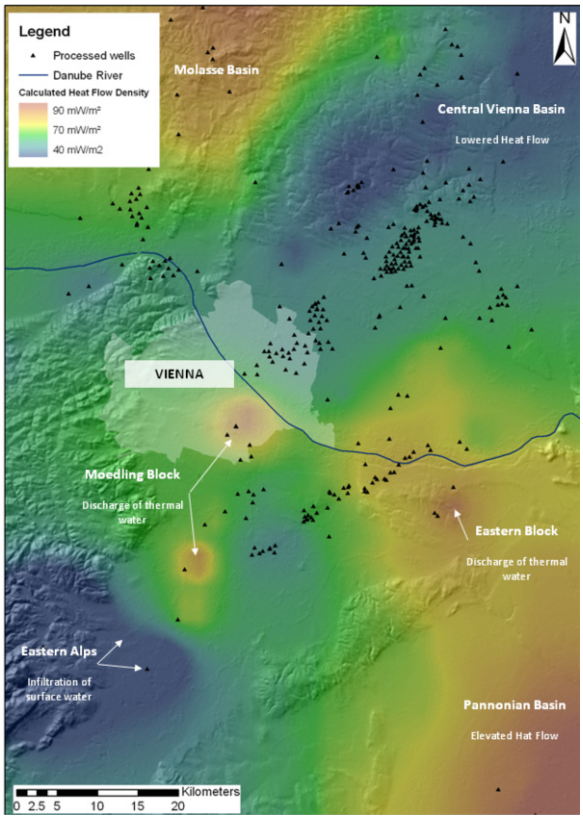

Figure 10: Surface heat flow density (HFD) in the region of the Vienna Basin based on processed borehole temperatures after low-pass filtering (weighted averaging, distance 10 km).

The pattern of modeled surface heat flow densities (Figure 10) indicates 5 different zones of geothermal condition: The transition zone between the southern Vienna Basin and the Pannonian Basin (1) is marked by successively increasing HFD values up to more than 100mW/m² as a result of generally enhanced geothermal conditions at the Pannonian Basin due to crustal thinning. Slightly enhanced HFD values are also shown at the transition zone between the Molasse Basin and the central Vienna Basin toward northwestern direction (2) exhibiting HFD values up to 85mW/m². This may be seen as a result of the combined effects of crustal stabilizing toward the Paleozoic shield of the Bohemian Massif and locally spread thermal water circulation systems at the basement of the Molasse Basin (permeable Jurassic limestones and Cretaceous clastic layers). The Northern Calcareous Alps situated at the southwestern part of the investigation area (3) are marked by significantly lowered geothermal conditions showing HFD values down to 40mW/m². The decrease of observed heat flux is understood to be influenced by crustal stacking by thrusting of Alpine units, combined with intense surface water inflow at highly permeable carbonatic nappes. A further zone of decreased geothermal conditions has been observed at the central and north-eastern parts of the Vienna Basin (4), which contain the largest depocenters (Schwechat depression, Zistersdorf depression) showing basin depths of up to 7000 meters. Although not yet totally examined a cooling effect by rapid deposition of cold surface sediments, mostly of upper Miocene and lower Plio-

cene age leading to non steady state geothermal conditions may be assumed as reason for a continuously decrease of observed HFD values down to 50 mW/m².

Despite of the previously presented large scale geothermal structures, several locally confined positive heat flux anomalies are observed at the already mentioned Moedling Block of the southern Vienna Basing showing maximum HFD values of up to 115mW/m². These anomalies are related to local discharge areas of the thermal water systems of the Moedling Block. The so far greatest geothermal anomaly is situated at the so called “Oberlaa High” at the south-eastern part of Vienna, exhibiting water temperatures of more than 50 degC at depths of 500 meter below surface.

5.4 Error Analyses of Model Parameters

Concerning subdomain parameters the effective thermal conductivity as well as the hydraulic permeability mark the most sensitive rock values having a great impact on the quality of model interpretation. As already mentioned interpretation and model recalibration mainly found on residuals between modeled and measured subsurface temperatures. While the data range of hydraulic permeabilities has been derived from measured data (drilling cores, hydraulic drill stem tests) the allocation of heat conductivities mainly bases on synthetic models, which are successively validated and recalibrated by laboratory measurements.

In order to obtain a preliminary quality check of modeled thermal conductivities a comparison with measured conductivities applied on 40 dry samples from geological units of both Neogene basin sediments as well as basement layers has been conducted (q.v. Figure 11).

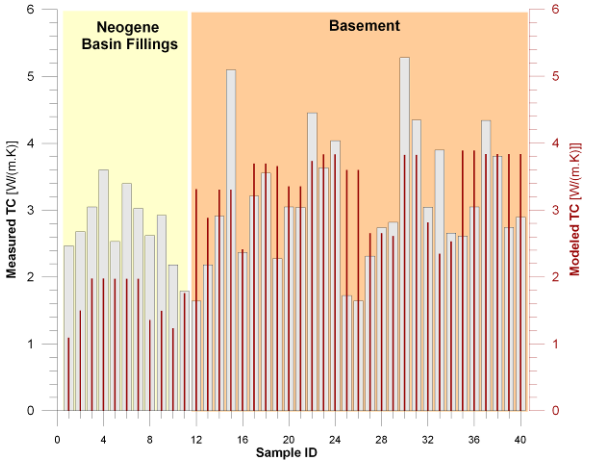

Figure 11: Comparison of modeled (red lines) and measured effective thermal conductivities (TC) for dry samples (air filled pores) at an ambient temperature of 25 degC.

The observed median aberration between measured and modeled data is in the range of 28%. In general the established models led to an underestimation of effective thermal conductivities at porous basin sediments, which is associated to an inadequate prediction of rock porosities, which in turn show a high sensitivity due to an enhanced conductivity contrast between rock mass and air filling. In opposite to this the average aberration between measured and modeled thermal conductivities is significantly lowered at barely porous basement rocks (~ 15%). It is evident, that observed residuals will be further decreased assuming water filled rock pores (lower conductivity contrast between rock mass and pore fillings).

Concerning the initial and boundary conditions of the aimed coupled thermal – hydraulic 3D modeling temperature conditions at the surface and base of the model are rather insensitive to the quality of the simulation itself. Basal heat flow densities (HFD) will be refitted iteratively in order to adjust measured subsurface temperatures in a first approach. The computed HFD will not be interpreted for identification of hydraulic flow. The surface temperatures in turn are well known for the Vienna Basin by empiric observations in shallow wells.

It is assumed, that the available temperature information, mainly gained from hydrocarbon exploration wells mark the most critical model parameter. The more so as the aimed interpretation of the coupled thermal – hydraulic simulation will base on observed residuals between modeled and measured subsurface temperatures (execution of analyses based on calculated Peclet Numbers).

6. DISCUSSION

6.1 Interpretation of Preliminary Results

The chosen geometrical units of the described volumetric 3D model at regional scale (model area approx. 50 x 60 km) is not capable to describe the entire thermal water systems of the southern Vienna Basin and clearly focuses on a target area situated at the western part (Moedling Block). A more complex, higher resolutive geometrical model is not able to be dealt with in a numerical way. Due to circumstance, that available input data for geometrical modeling are distributed quite unevenly and due to the fact, that profound seismic data are widely lacking the achieved volumetric model will be fault-prone especially at the south-western part. This urges the need for plausibility check-ups, which will be achieved by an additional alternative interpolation algorithm.

The petrophysical data-models, which will be build up independently of the volumetric model are designed to be flexible and changeable after accomplishment of the first simulation circles. Most of the used start-up models are designed statically based on averaged values. It is assumed that depth dependence of the total pore fraction will lead to aberrational results especially at highly overburdened Neogene sediments, which was already indicated at the comparison of modeled and measured thermal conductivities (q.v. Figure 11). Considering the hydraulic permeability of deep sedimentary and basement units of the Southern Vienna Basin enhanced conditions are indicated at the top of the basement, which are linked to previous exposure, karstification and erosion, which lead to the evolution of clastic layers at the base of the Neogene basin filling. Model unit B2, which is dominated by massive Triassic dolomites exhibits several highly permeable zones up to more than 1000 meters below the top of the generalized unit. Nevertheless further structural analyses based on geophysical well data are needed to focus high permeable zones, especially linked to fault systems.

Preliminary geothermal analyses based on pure conductive 1D modeling show, that the Southern Vienna Basin is situated at the transition zone between low to moderate geothermal conditions at the Alpine mountains and clearly elevated heat flow densities at the region of the Pannonian Basin. A successive decrease of observed HFD values toward the north-eastern part of the Vienna Basin indicates geothermal patterns, which are assumed to be linked to changing structural conditions. One possible explanation of the achieved observation is given by non-steady state condi-

tions due to rapid sedimentation of cold surface sediments. Further analyses are needed to prove this assumption.

6.2 Strength and Limitation of Chosen Approach

The chosen approach was designed in order to allow geothermal 3D analyses at regions with lacking detailed seismic data. The scattered and heterogeneous geometrical and geophysical input-data constitute a great challenge for reservoir modeling. The main advantage of the presented approach is given by flexible data-models which are iteratively adapted by forward modeling (coupled thermal – hydraulic 3D simulation circles) in combination with inverse methods to provide information for no-data areas within the investigation area. It has to be kept in mind that the presented study is executed at a regional scale and intends to establish a data fundament for later detailed modeling at distinguished sites within the investigation area.

The quality of the designed method is strongly depending on the quality of thermal calibration data, which are provided by BHT- and DST datasets. The more so as observed residuals between measured and modeled subsurface temperatures are going to be transformed into Peclet numbers inaccuracies according to temperature measurements constitute the most limiting constraint of the proposed approach.

6.3 Outlook on Further Activities

Despite of the aimed coupled thermal – hydraulic 3D modeling, which is described at chapter 4.5, further preparing analyses are necessary. The preliminary data-model of hydraulic permeabilities, which currently rely on unevenly distributed borehole measurements have to be specified using continuous geophysical logging data and hydrochemical data, which have not been processed yet. Beside, the actual purely synthetically model of thermal conductivities has to be further calibrated based on petrophysical laboratory measurements.

7. CONCLUSION

The presented paper treads a combined empiric – synthetic approach in order to establish 3D reservoir modeling at the absence of detailed seismic data. To reach this goal model calibration and interpretation strongly relies on observed residuals between measured and modeled borehole temperatures. The chosen approach offers possibilities at an environment of scattered and low-quality subsurface data, but in turn strongly depends on the quality of available temperature information. Due to the circumstance, that the presented study is still undergoing, the actual paper has to focus on pre-modeling research activities.

8. NOMENCLATURE

λ_s	Thermal conductivity of solid rock matrix [W/(m·K)]
$\lambda_{s,i}$	Thermal conductivity of individual rock-types
$c_{p,s}$	Specific (isobarometric) heat capacity of solid rock matrix [J/(kg·K)]
$c_{p,s,i}$	Specific (isobarometric) heat capacity of specific rock type
n_i	Normalized volumetric weight [-]
λ_f	Thermal conductivity of pore fluid
$c_{p,f}$	Specific heat capacity of pore fluid
ρ_f	Density of pore fluid [kg/m³]
λ_{eff}	Effective (bulk) thermal conductivity of specific stratum
$c_{p,eff}$	Effective (bulk) heat capacity of specific stratum
Φ_b	Bulk porosity [-]
κ	Effective bulk thermal diffusivity (drilling mud and surrounding rock mass) [m²/s]
a	Radius of well [m]
T_{Form}	True formation temperature [°C]
$\Delta T'$	Initial thermal perturbation related to circulating mud [°C]
t	Shutdown period of well [s]
q	Terrestrial heat flow density [W/m²]
m_i	Thickness of the i-th stratum of a layered half-space [m]
T_i	Formation temperature at the base of the i-th stratum [°C]
l	Effective hydraulic thickness [m]
$v_{D,z}$	Effective Darcy velocity, projected at vertical direction [m/s]

ACKNOWLEDGEMENT

The presented study is financed by the Austrian Academy of Science and the government of Lower Austria. Special thanks have to be given to OMV AG for providing essential borehole temperatures and petrophysical data.

REFERENCES

Brix F. and Schultz O. (Eds.), 1993: Erdöl und Erdgas in Österreich, 2nd edition, Naturhistorisches Museum, Wien.

Calcagno, P., Chiles, J.P., Courrioux, G. And Guillen, A., 2008: Geological modelling from field data and geological knowledge: Part I. Modelling method coupling 3D potential-field interpolation and geological rules, Physics of the Earth and Planetary Interiors, 171, 1-4, pp. 147-157.

Faupl, P., 2003: Historische Geologie, 2nd edition, Facultas Verlags- und Buchhandels AG, Vienna.

Fertl W. H., Wichmann P. A., 1979, How to determine static BHT from well log data, World Oil, Vol. 184 pp. 105 – 106.

Kroell A. (ed.), 1993: Geologische Themenkarten der Republik Österreich - Wiener Becken und angrenzende Gebiete 1:200.000, Geological Survey of Austria, Vienna.

Kohl T., Hopkirk R.J., 1995: "FRACTure"-A simulation code for forced fluid flow in fractured, porous rock, Geothermics 24, p. 333 – 343.

Kutasov I.M., 1999: Applied geothermics for petroleum engineers, Developments in Petroleum Science Vol. 48, Elsevier.

Lachenbruch A.H., Brewer M. C., 1959: Dissipation of the temperature effect of drilling a well in Arctic Alaska, Geological Survey Bulleti, Vol. 1083, pp. 73 – 109.

Leblanc Y., Pascoe L. J. Jones F.W., 1981: The temperature stabilization of a borehole, Geophysics, Vol. 46, pp. 1301 – 1303.

Sass J.H., Lachenbruch A.H., Moses T.H., 1992: Heat flow from a scientific research well at Cajon Pass, California, J. Geophys. Res. Vol. 97, pp. 5017 – 5030.

Schoen J., 1983: Petrophysik – Physikalische Eigenschaften von Gesteinen und Mineralien, Akademie Verlag Berlin.

Schnabel W. (ed.), 2002: Geologische Karte von Niederösterreich 1:200.000, Geological Survey of Austria, Vienna.

Wessely G., 1983: Zur Geologie und Hydrodynamik im südlichen Wiener Becken, *Mitteilungen ÖGG* Vol. 76, pp. 27-68, Wien.

Wessely, G., (ed.), 2006: Geologie von Niederösterreich, Geological Survey of Austria, Vienna.

Zoetl J., Goldbrunner J., (1993): Die Mineral- und Heilwässer Österreichs, Springer-Verlag Wien.